Vibrational relaxation of bulk modes perturbed by electronic state of dilute impurities

Ta-Chau Chang,[a] Shiow-Hwa Chou, and Hung-Wen Li[b]
Institute of Atomic and Molecular Sciences, Academia Sinica, P.O. Box 23-166, Taipei, Taiwan, 10764, Republic of China

Sheng-Hsien Lin
Department of Chemistry and Biochemistry, Arizona State University, Tempe, Arizona 85287-1604

Vibrational dephasing of the 1385 cm^{-1} vibron of host molecules (naphthalene) perturbed by electronically excited guest molecules (pentacene) was studied by the time-resolved coherent Stokes Raman spectroscopy (CSRS) in the temperature region of 6–26 K. The decay time was faster when the excitation frequency was tuned from the off-resonance to the resonance of the electronic transition of pentacene. For the resonance case, longer decay times were observed at higher temperatures (~ 26 K) than at low temperatures (~ 6 K). Two possible mechanisms were considered for the inverse temperature behavior. The shorter decay time in the impurity perturbed domains may be attributed to the increase of a coupling strength on the decay channel from 1385 cm^{-1} mode to 1365 cm^{-1} mode by stimulating phonon emission.

I. INTRODUCTION

The excitation of a guest molecule suspended in a molecular crystal can be transferred to a nearby molecule by absorbing or emitting a phonon via the coupling of guest electronic states and host phonon states (the electron–phonon coupling). Linear electron–phonon coupling produces the phonon sideband in the absorption and emission spectra, while quadratic coupling is responsible for the broadening and shifting of the impurity zero-phonon bands.[1-6] In a mixed molecular crystal, there are three types of phonons: acoustic and optical phonons which are the lattice motions of the bulk crystal and a pseudolocal phonon which can be attributed to the coupling of the localized guest states with bulk phonons.[7-9] In general, coupling to a pseudolocal phonon is a dominant mechanism for optical dephasing in molecular crystals at low temperature.[9,10] However, to our knowledge no attempt has been made to study how the electron–phonon coupling affects the vibrational relaxation of host vibrons in a mixed crystal.

Time-resolved coherent anti-Stokes Raman spectroscopy (CARS) has been employed to measure the vibrational relaxation in mixed molecular crystals for a better understanding of the vibrational dynamics in solid state chemistry.[11-18] Fayer and co-workers[17] used the time-resolved CARS method to probe the coupling between impurity electronic states and bulk phonons. They found that shorter decay time on resonance and normal decay time off resonance. In addition, the signal was resonantly enhanced by a factor of 10 in intensity. Their results were interpreted in terms of impurity perturbed domains (IPD).[17] The enhancement of signal is attributed to the resonantly enhanced nonlinear susceptibility of the phonon in IPD via

electron–phonon coupling. However, no detail mechanism was given for the short decay time on resonance. The objective of this work is to examine how the impurity excitation affects the decay processes of host vibrons and why the decay arising from the IPD is faster based on the temperature dependence study.

We have measured the decay times of the 1385 cm^{-1} vibron of naphthalene (NPH) in the mixed crystals of pentacene (PT) doped in NPH molecular crystals by using both on-resonant and off-resonant time-resolved CSRS over a temperature range from 6 K to 26 K. For the off-resonance case, the decay times are independent of temperature in this temperature range. However, longer decay times are observed at higher temperatures (~ 26 K) than at low temperatures (~ 6 K) in the on-resonance spectra. The experimental data are interpreted in terms of the IPD model. The interplay between the IPD domains and the bulk domain may be able to explain the inverse temperature behavior. In addition, it is found that the inverse temperature effect on vibrational relaxation has been predicted based on the adiabatic approximation model of vibrational relaxation of impurity molecules in solids.[19-22] This model can be used to describe the inverse temperature results. The temperature dependence of vibrational relaxation provides an important insight into the faster decay times in the IPD model.

II. EXPERIMENT

The ps CSRS experimental apparatus was described previously.[18] An acousto-optically mode-locked and Q-switched Nd:YAG laser (Coherent Antares-76) was used to generate a pair of homemade sync pump dye lasers. The dye laser emitted trains of ≈ 10 pulses separated by 13 ns at repetition rate of 500 Hz. The average power is ≈ 50 mW and the pulse width is ≈ 30 ps measured by autocorrelation function. In the ps CSRS process, a simultaneous pulse pair of ω_1 and ω_2 coherently excited a vibration mode

---

[a]To whom correspondence should be addressed.
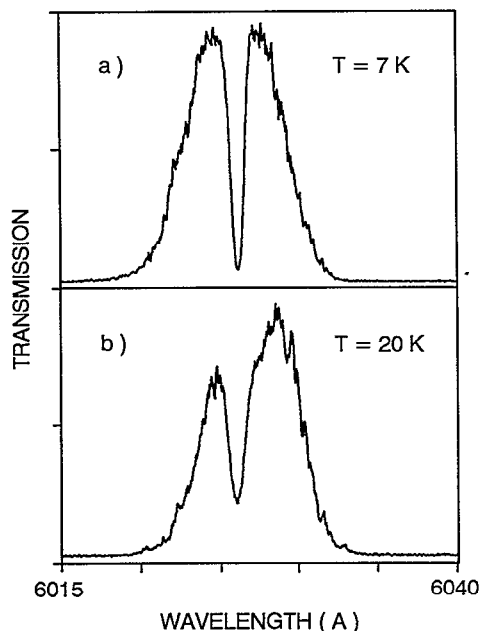[b]Department of Chemistry, National Taiwan University, Taipei, Taiwan, ROC.

FIG. 1. Temperature-dependent absorption spectra of zero-phonon band of pentacene doped in naphthalene. The spectra are obtained from the same spot by locating a broad band laser at the absorption frequency of PT and scanning a monochromator from 6015 Å to 6040 Å at (a) $T=7$ K, and (b) $T=20$ K.

FIG. 2. Temperature-dependent time-resolved CSRS spectra for the 1385 cm^{-1} vibron of NPH in the PT/NPH mixed crystals. (a) Off-resonance at 7 K, (b) off-resonance at 23 K, (c) on-resonance at 7 K, and (d) on-resonance at 23 K. The insets show their semilog plots of ps CSRS decay.

at ω_{v0}, where $\omega_2 - \omega_1 = \omega_{v0}$. The subsequent decay of vibrational coherence was monitored by a time-delayed pulse ω_1. The CSRS signal at $2\omega_1 - \omega_2$ was spatially filtered by an aperture and frequency filtered by a Jobin Yvon THR-1000 spectrometer. The change of intensities at the CSRS probes was detected by a photomultiplier and a lockin amplifier. The experimental data were processed by a personal computer. The results represent the average of ten scans.

The PT/NPH mixed crystals at various concentrations of PT were grown by Bridgman furnace. NPH was extensively zone refined and PT was only vacuum sublimed prior to use. Crystals were cleaved parallel to the ab plane. Crystal thickness (L) was varied from 0.2 to 0.8 mm. Samples with clear transparency were mounted in a flat brass plate in a Janis liquid helium cryostat. The temperature was measured by a calibrated silicon diode temperature sensor (Lake Shore Cryotronics model). Since PT may not be microscopically uniform in these samples, it is difficult to obtain the exact values of concentration. We have measured the optical density (OD) on the spot where the CSRS data are taken. The spot size on the sample is 180 ± 20 μm. The resonant transition is found by locating a broad band laser with FWHM of ~5 Å at the absorption of PT and scanning a monochromator to find a minimum transmission and then inserting a 100 μm etalon to narrow the laser bandwidth to <2 cm^{-1}. A typical absorption spectrum for measuring the OD is shown in Fig. 1. The magnitude of OD/L can be deviated by as large as $\pm30\%$ for the crystals with higher concentration of PT. It is noted that the energy of pump pulse is four times stronger than the energy of probe pulse for all the CSRS spectra. In every
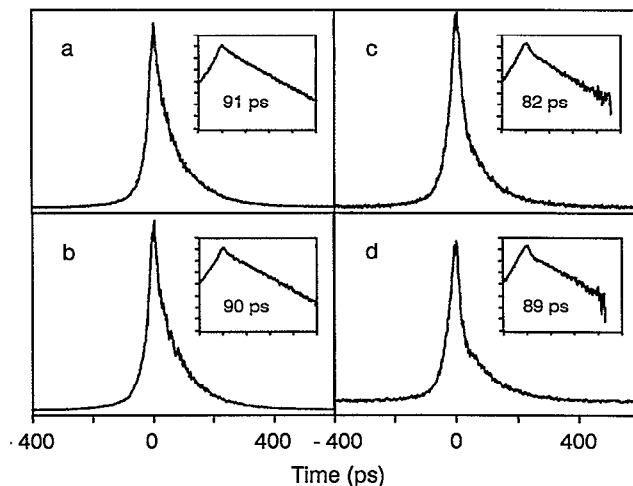
case, we were very careful to examine if the sample was damaged.

III. RESULTS AND DISCUSSION

Figure 2 shows temperature-dependent spectra of the 1385 cm^{-1} vibron of NPH in the PT/NPH mixed crystals under the perturbation of the electronic excitation of PT at different excitation frequencies. The insets in Fig. 2 show the semilog plot of decay curve. The decay time of the off-resonance case at a temperature of 7 K is identical to that at 23 K, and is similar to that observed in pure NPH crystals. The decay times measured in pure NPH crystals are nearly temperature independent up to $T\approx40$ K.[18,23,24] However, Figs. 2(c) and 2(d) show that the decay time of the on-resonance case is shorter at low temperature (7 K) than at high temperature (23 K). This effect is shown more clearly in Fig. 3. Their decay times measured from the slopes of two converging lines are 83 ± 3 ps and 95 ± 2 ps at 6 K and 26 K, respectively. The decay times measured from three different crystals at different temperatures are summarized in Table I. It is quite clear that the decay time increases with increasing temperature.

The shorter decay time of the on-resonance case than that of the off-resonance case as shown in Fig. 2 has been previously described in terms of impurity perturbed domains.[17,25] In the IPD model,[17] two active oscillators, $X^{(3)}$(NPH) and $X^{(3)}$(IPD), contribute additively to the nonlinear susceptibility $X^{(3)}$. Without including the nonresonant background, the $X^{(3)}$ is given as

$$X^{(3)} = X^{(3)}(\text{NPH}) + X^{(3)}(\text{IPD}),\tag{1}$$

where $X^{(3)}$(NPH) is identical to that in the neat crystals and $X^{(3)}$(IPD) is the bulk modes admixed with impurity electronic character via electron–phonon coupling. The
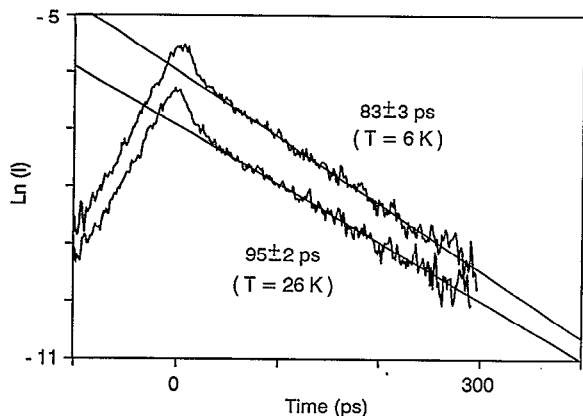
FIG. 3. Semilog plots of the time-resolved CSRS decay at two different temperatures, 6 K (top) and 26 K (bottom). The decay gets slower at high temperature (26 K) than at low temperature (6 K). The lines are for visual guides.

FIG. 4. Energy diagram of a four level system for the multiresonant time-resolved CSRS.

susceptibilities $X^{(3)}$(NPH) for simple CSRS and $X^{(3)}$(IPD) for the multiresonant CSRS in a four-level system as shown in Fig. 4 are given as[26–29]

$$X^{(3)}(\text{NPH}) = A[1/(\omega_{0v} - \Delta + i\Gamma_{0v})], \tag{2}$$

$$X^{(3)}(\text{IPD}) = B[1/(-d + \omega_{0v} - \Delta + i\Gamma_{0'v}) \times \{1/(\omega_{0'v'}$$
$$- \Delta + i\Gamma_{0'v'})(d + \omega_{0'v'} - \Delta + i\Gamma_{0v'})$$
$$+ 1/(\omega_{0v} - \Delta + i\Gamma_{0v})(d + \omega_{0'v'} - \Delta + i\Gamma_{0v'})$$
$$+ 1/(\omega_{0'v'} - \Delta + i\Gamma_{0'v'})(-d + i\Gamma_{0'0})\}], \tag{3}$$

where $|0\rangle$ and $|0'\rangle$ correspond to the ground and excited electronic states and $|v\rangle$ and $|v'\rangle$ denote their vibrational states, respectively. Here Γ_{ij} is the damping parameter, $\Delta = \omega_1 - \omega_2$, $\omega_s = 2\omega_1 - \omega_2$ ($\omega_1 < \omega_2$), and $d = \omega_{0'0} - \omega_1$, which is the detuning parameter. A and B are proportional to the transition moments. It should be noted that the transition moment in $X^{(3)}$(IPD) takes into account the electron–phonon coupling. The existence of the coupling is confirmed by the presence of the phonon sideband.[9] The only coupling terms enhanced are those associated with specific wave vectors due to the coherent excitation. Thus, $X^{(3)}$(IPD) can be dominant when d is zero and $X^{(3)}$(NPH) is dominant when d is large. It is clear that the concentration of pentacene guest molecules will affect the relative importance of the contributions $X^{(3)}$(IPD) and $X^{(3)}$(NPH) to the signal. This behavior can be found in Table I, which the decay times depend slightly upon the
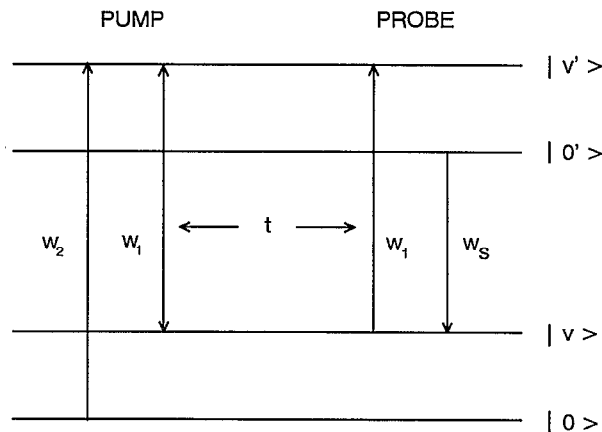
magnitude of OD/L. The concentration effect has been discussed in our previous paper.[25] It is suggested that the IPD model can be used to describe our experimental results.

Since the decay time in the near crystals is 95 ± 5 ps, the shorter decay time of the on-resonance case as shown in Fig. 2(c) should be the decay time of vibron in the impurity perturbed domains. Single exponential decay over a range of three factors of e suggests that the contribution from $X^{(3)}$(NPH) to the on-resonance spectra is negligible and the guest molecules of PT are uniformly embedded in the host crystals of NPH. If the two contributions are comparable, nonexponential decay would be expected. The nonexponential decay presented in Fig. 5 is taken from a thick crystal under the resonant condition at $T = 7$ K. The IPD model predicts that a thin crystal with a high PT concentration exhibits a single exponential decay, while a thick crystal with a low PT concentration exhibits a nonexponential decay.[17] This is because the relative number of bulk oscillators is larger for the latter. It should be noted that Figs. 3 and 5 are obtained from the samples with different OD/L. Thus, their decay times are somewhat different. We suggest that the two contributions to the CSRS signal described in the IPD model may be the cause of the nonexponential decay presented in Fig. 5. However, the strain effect remains a possible cause for the nonexponential decay. In addition, the possibility of a variety of impurity domain types is not considered. A systematic study of the effect of sample thickness and concentration is in progress.

We now turn our attention to the temperature effect on the short decay time. It is known that the increase of the

TABLE I. Temperature-dependent decay times of the 1385 cm^{-1} vibron of NPH in the PT/NPH mixed crystals while tuning ω_1 into the electronic transition of PT.

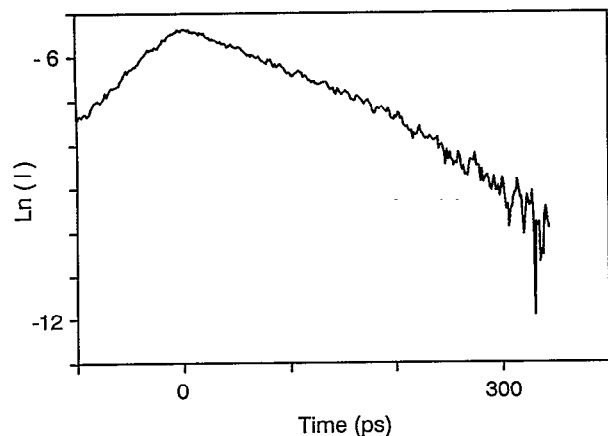| Crystal	1	2	2	3	3
OD/L	1.5	2.5	2.5	1.4	1.2
decay time (ps)	79 ± 3 (7 K)	73 ± 2 (6 K)	72 ± 3 (7 K)	82 ± 2 (7 K)	83 ± 3 (6 K)
	88 ± 3 (19 K)	83 ± 3 (16 K)	84 ± 3 (24 K)	89 ± 3 (23 K)	95 ± 2 (26 K)

FIG. 5. Example of a nonexponential CSRS decay of the 1385 cm^{-1} vibron in a mixed crystal.

contribution from IPD domains decreases the decay time. At low temperatures the linewidth of the zero-phonon line is ≈ 2.5 cm^{-1} which is shown in the central dip of Fig. 1(a), and which is approximately equal to the bandwidth of the excitation pulses. Thus, the entire inhomogeneous lines are coherently excited. At higher temperatures the zero-phonon line is weaker and broader due to thermal broadening as shown in Fig. 1(b), and impurities are only partially excited. Since the IPD resulting from electron–phonon coupling is closely connected to the number of impurity domains, the contribution from IPD to the CSRS signal is prominent at low temperatures. Thus, highly excited IPD at low temperature provides means for a faster decay. Therefore, shorter decay time at low temperature and longer decay time at high temperature may be attributed to the interplay between the IPD domains and the bulk domain. If this is the case, the nonexponential decay should be observed at medium temperature. Although the temperature dependent spectra show the decay more like single exponential, this mechanism cannot be excluded since the difference of the decay times between $T = 6$ K and $T = 26$ K is ~ 10 ps. It should be emphasized that electron–phonon coupling would only affect the number of impurity domains, it does not determine the vibrational relaxation. The question is what the mechanism for the inverse temperature effect is if the decay is a single exponential.

Theories of vibrational relaxation of impurity molecules in solids have been developed by Diestler, Jortner, and Lin.[19–22] The inverse temperature dependence of vibrational relaxation can be treated by using the adiabatic approximation model.[19] In this theory, the frequencies of the vibrons are much larger than those of the phonons so that the adiabatic type of approximation can be used to separate the Hamiltonian into the vibron motion and phonon motion.[19] The vibrational relaxation is determined by the coupling between vibron and phonon motion. This coupling is similar to the Born–Oppenheimer (BO) coupling in the electronic relaxation.[30] The coupling constant (or the Huang–Rhys factor) S is given by[31]

$$S = \sum_i (1/2)\beta_i^2 \, \Delta Q_{vv'}^2 \, \coth(\hbar\omega_i/2kT)$$

$$= \sum_i S_i \coth(\hbar\omega_i/2kT), \tag{4}$$

where $\Delta Q_{vv'}$ is related to the anharmonic couplings between vibron and phonon.[19] Since it is difficult to determine all the modes involved in the summation of equation, an average frequency, ω_P, is introduced for reducing Eq. (4) to

$$S = \sum_i S_i \coth(\hbar\omega_P/2kT)$$

$$= S_0 \coth(\hbar\omega_P/2kT) = S_0[2n_P(T) + 1], \tag{5}$$

where S_0 is the coupling strength at $T = 0$ K and $n_P(T)$ is the thermal occupation numbers of phonon states, $n_P(T) = [\exp(\hbar\omega_P/k_B T) - 1]^{-1}$. Using the adiabatic wave functions as a basis set and the BO coupling as the perturbation, the temperature effect on the vibrational relaxation can be derived and is given as[19]

$$\tau(0)/\tau(T) = \exp[-2S_0 \, n_P(T)][n_P(T) + 1]^N$$

$$\times \sum_m [N!/m!(m+N)!][S_0^2 \, n_P(T)$$

$$\times (n_P(T) + 1)]^m, \tag{6}$$

where $N = (\omega_V - \omega_A)/\omega_P$. Depending on S_0 and ω_P, Eq. (6) exhibits both normal and inverse temperature effects.

According to the IPD model,[17] the 1385 cm^{-1} mode of a host molecule near the impurity molecule is excited due to the intermolecular electron–phonon interaction between the host and impurity molecules. This particular host molecule would have different local modes from those of the bulk host molecules. Thus, the vibrational relaxation of the host molecule in the IPD can be regarded as that of an impurity molecule. Therefore, we can use Eq. (6) to describe our results. Figure 6 shows the temperature effect on vibrational relaxation based on Eq. (6). For comparison, three sets of experimental data are given in Fig. 6. In Fig. 6, we assume that $N = 1$. It is found that small value of ω_P favors the inverse temperature behavior. Considering the phonon density of state in the neat NPH crystal,[32] the set of parameters $S_0 \approx 0.8$ and $\omega_P \approx 20$ cm^{-1} can fit our experimental results. Considering that this is an approximation model and that the temperature range covered by the data is not large, the agreement between experiment and theory appears reasonable.

Temperature dependence study may unravel why the decay arising from the IPD is faster. Ranson and co-workers[33] have suggested that the possible decay channels for the 1385 cm^{-1} mode involve either two vibrons or one vibron and one phonon. As we do not have enough information for calculating the two-vibron processes, we are not able to calculate the decay time for this mode. However, one of the possible decay channels of the 1385 cm^{-1} mode in the neat NPH crystal involving a vibron at 1365 cm^{-1} and a lattice phonon at 20 cm^{-1} via the cubic anharmonic
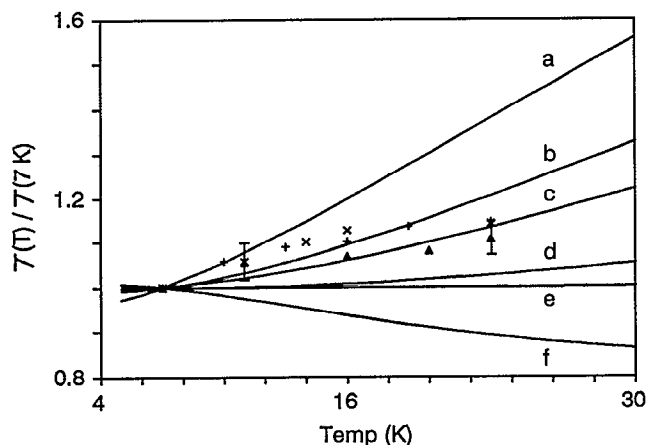
FIG. 6. The plots of $[\tau(T)/\tau(7 \text{ K})]$ vs temperature for the three sets of data $(\times, \triangle, +)$. For clarity only two error bars are displayed. The six solid lines are calculated by using $N=1$ for all curves based on Eq. (6). The value of (S_0, ω_P) are given for the curve a: (0.8,10), b: (1.0,20), c: (0.8,20), d: (0.8,40), e: (0.8,100), and f: (0.3,20), respectively.

coupling is most interesting.[24,33] The coincidence of the coupling phonon frequency involved in this decay channel and the average phonon frequency obtained in the temperature dependence study implies that this decay channel may be responsible for the inverse temperature behavior when the impurity is excited.

In addition, the 20 cm^{-1} is also approximately identical to the frequency of the pseudolocal phonon mode reported by Hesselink and Wiersma.[9] They have found a peak superimposed on a broad phonon sideband at ~36 cm^{-1} in the emission from the PT/NPH mixed crystals. The temperature dependence of the decay is exponentially activated with the activation energy approximately half of the energy observed in the sideband. They assigned this band to be the $2 \leftarrow 0$ transition of a pseudolocal phonon mode. The pseudolocal phonon energy of the $1 \leftarrow 0$ transition is 18 cm^{-1}, which can couple to the acoustic phonon branch. They concluded that the pseudolocal phonon mode is responsible for the dephasing of the zero-phonon line. The approximate coincidence of these phonon frequencies leads us to the conjecture that the increase of phonon distribution at 20 cm^{-1} due to the impurity excitation is responsible for the shorter decay time of the on resonance case. Mode specific effects may be able to answer this question, which are currently being examined.

In summary, we have studied vibrational dephasing of the 1385 cm^{-1} vibron of host molecule (NPH) perturbed by an electronically excited guest molecule (PT) using the time-resolved CSRS method. Shorter decay times were observed when the excitation energy was tuned to the electronic transition of the guest molecule and the vibrational decay time exhibits inverse temperature dependence. This behavior is consistent with the IPD model. The possible

mechanisms for the inverse temperature effect on decay time were discussed. We have further proposed that the shorter decay time in IPD is attributed to the increase of the decay process from 1385 cm^{-1} mode to 1365 cm^{-1} mode by stimulating phonon emission.

ACKNOWLEDGMENTS

[1] D. Hsu and J. L. Skinner, J. Chem. Phys. **81**, 1604 (1984).
[2] J. L. Skinner and D. Hsu, Adv. Chem. Phys. **65**, 1 (1986).
[3] R. H. Silsbee, Phys. Rev. **128**, 1726 (1962).
[4] D. E. McCumber and M. D. Sturge, J. Appl. Phys. **34**, 1682 (1963).
[5] A. A. Maradudin, Solid State Phys. **18**, 273 (1966).
[6] I. S. Osad'ko, in *Spectroscopy and Excitation Dynamics of Condensed Molecular Systems*, edited by V. M. Agranovich and R. M. Hochstrasser (North-Holland, Amsterdam, 1983).
[7] G. J. Small, Chem. Phys. Lett. **57**, 501 (1978).
[8] P. de Bree and D. A. Wiersma, J. Chem. Phys. **70**, 790 (1979).
[9] W. D. Hesselink and D. A. Wiersma, J. Chem. Phys. **73**, 648 (1980).
[10] R. W. Olson, J. S. Meth, C. D. Marshall, V. J. Newell, and M. D. Fayer, J. Chem. Phys. **92**, 3323 (1990).
[11] F. Ho, W.-S. Tsay, J. Trout, S. Velsko, and R. M. Hochstrasser, Chem. Phys. Lett. **97**, 141 (1983).
[12] S. Velsko and R. M. Hochstrasser, J. Chem. Phys. **82**, 2180 (1985).
[13] E. L. Chronister and D. D. Dlott, J. Chem. Phys. **79**, 5286 (1983).
[14] E. L. Chronister, J. R. Hill, and D. D. Dlott, J. Chim. Phys. **82**, 159 (1985).
[15] K. Duppen, D. P. Weitekamp, and D. A. Wiersma, J. Chem. Phys. **79**, 5835 (1983).
[16] D. P. Weitekamp, K. Duppen, and D. A. Wiersma, Phys. Rev. A **27**, 3089 (1983).
[17] W. L. Wilson, G. Wackerle, and M. D. Fayer, J. Chem. Phys. **87**, 2498 (1987).
[18] T.-C. Chang, B. H. Jou, R. S. Ou, C. C. Chiang, and H. W. Li, Chem. Phys. Lett. **187**, 208 (1991).
[19] S. H. Lin, J. Chem. Phys. **65**, 1053 (1976).
[20] S. H. Lin, J. Chem. Phys. **44**, 3759 (1966).
[21] D. J. Diestler, J. Chem. Phys. **60**, 2692 (1974).
[22] A. Nitzan, S. Mukamel, and J. Jortner, J. Chem. Phys. **63**, 200 (1975).
[23] D. D. Dlott, C. L. Schosser, and E. L. Chronister, Chem. Phys. Lett. **90**, 386 (1982).
[24] C. L. Schosser and D. D. Dlott, J. Chem. Phys. **80**, 1394 (1984).
[25] T.-C. Chang, T. Y. Liu, H. M. Wu, and H. W. Li, Chem. Phys. Lett. **197**, 476 (1992).
[26] N. Bloembergen, H. Lotem, and R. T. Lynch, Indian J. Pure Appl. Phys. **16**, 151 (1978).
[27] T.-C. Chang, C. K. Johnson, and G. J. Small, J. Phys. Chem. **89**, 2984 (1985).
[28] J. R. Andrews and R. M. Hochstrasser, Chem. Phys. Lett. **82**, 381 (1981).
[29] T.-C. Chang Ph.D. Thesis, Iowa State University, 1985.
[30] M. Born and R. Oppenheimer, Ann. Phys. **84**, 457 (1927).
[31] M. Born and K. Huang, *Dynamics Theory of Crystal Lattice* (Oxford University, New York, 1954).
[32] A. V. Belushkin, E. L. Bokhenkov, A. I. Kolesnikov, I. Natkaniec, R. Righini, and E. F. Sheka, Sov. Phys. Solid State **23**, 1529 (1981).
[33] P. Ranson, R. Ouillon, and S. Califano, Chem. Phys. **86**, 115 (1984).